Analysis of influence of nonlinearities and noise correlation time in a single-DOF energy-harvesting system via power balance description

(Article begins on next page)

19 April 2024

Analysis of influence of nonlinearities and noise correlation time in a single DOF energy harvesting system via Power Balance description

Michele Bonnin · Fabio L. Traversa · Fabrizio Bonani

Abstract We discuss the role played by the time correlation properties of stochastic sources and by model nonlinearities in single degree of freedom energy harvesting systems. After transforming the state equations into energy-angle coordinates, we apply a stochastic projection operator technique to obtain the system power balance equation. The latter allows to evaluate both the magnitude of the power injected by noise into the system as well as the harvested power, thus providing a tool instrumental for designers to optimize the harvester. We show that for systems with modulated (multiplicative) noise, nonlinear energy harvesters can outperform their linear counterparts, highlighting the physical mechanism that explains their better performance.

Keywords Energy harvesting · white noise · colored noise · stochastic processes · stochastic differential equations · Fokker-Planck equation · nonlinear oscillators

1 Introduction

The rapid development of new technologies, e.g. the internet of things paradigm, poses new challenges. Among

Michele Bonnin
Dipartimento di Elettronica e Telecomunicazioni
Politecnico di Torino, Torino, Italy
E-mail: michele.bonnin@polito.it

Fabio L. Traversa
MemComputing Inc.
San Diego, CA, USA
E-mail: ftraversa@memcpu.com

Fabrizio Bonani
Dipartimento di Elettronica e Telecomunicazioni
Politecnico di Torino, Torino, Italy
E-mail: fabrizio.bonani@polito.it

many, a problem of paramount importance is how to supply power to networks of dispersed electronic and electro-mechanical apparatuses. Old fashioned answers, e.g. disposable batteries, are rarely a viable solution, because of their limited power density and life, not to mention the often practically impossible replacement once exhausted.

Alternative solutions have been proposed, such as electronic systems that can wirelessly exchange not only data but also power [1–3], or systems able to scavenge energy from the surrounding environment [4–6]. The second solution, known as *energy harvesting*, promises the realization of self-powered systems, or at least to expand the battery lifetime for those systems where continuous operation without maintenance is highly desirable [7,8]. Effective energy harvesting requires to design electronic or, more often, electro-mechanical systems able to collect the ambient energy where and when necessary, being the ultimate power source electromagnetic radiation, solar light, temperature gradients, or mechanical vibrations. When the power source is characterized by random phenomena, the corresponding energy harvester is termed stochastic.

The main limitation of stochastic energy harvesting systems is the low power density of environmental noise: however, although negligible on a macro scale, environment induced fluctuations may become significant at the micro scale. In this case, parasitic mechanical vibrations are particularly attractive, because of their almost ubiquitous presence and of their relatively high (at least when compared to other possible sources) energy density. Mechanical energy can be converted into electric power exploiting several different physical principles, such as piezoelectricity, electromagnetic induction or capacitance variations [9–11].

All these systems have in common the presence of an oscillator as transducer, in which the autonomous system proper frequencies have to be tuned to the spectral region where most of the energy is available. As well known, linear oscillators are *pass-band filters*, i.e. they are designed to work efficiently in a narrow frequency range centered around a specific value. Unfortunately, the energy of ambient vibrations is typically spread over a wide range of frequencies, with significant predominance of low frequency components, rather than being concentrated around a single frequency. The result is a low efficiency of the harvesting process, because only a small fraction of the available energy can be collected. Moreover, tuning the oscillator is not always an easy task due to geometrical constrains. In fact minimizing the generator to the nanoscale, the resonance frequency tends to increase up to kHz/MHz values, for which the vibration energy content is generally very small.

Devising solutions that increase the harvested power is a major goal. Several authors suggested that energy harvesters based on nonlinear oscillators can outperform linear ones, see e.g. [12–19]. In particular, nonlinear oscillators may exhibit a wider spectral response, and can be operated in such a way that their frequency response matches more closely the energy spectral contents available in the environment. Nonlinearities also play a fundamental role in system with multiplicative (modulated) noise. Multiplicative noise is ubiquitous in nature, the simplest example being Brownian motion in thermal environments: here amplitude fluctuations depend on temperature, that in turn depends on position. When one or more noise components are proportional to the state of the systems, nonlinearities may amplify fluctuations along certain directions, while dampening others. The result is a net non null contribution to expected quantities that may alter the energy balance, similarly to what happens to phase noise in nonlinear oscillators [20–22]

Recently, several techniques have been developed to investigate the dynamics and performance of energy harvesters. When the external power source is modeled by a simple periodic signal, harmonic balance techniques and bifurcation theory can be applied [23–25]. Conversely, if noise is modeled as a truly random signal, stochastic calculus is needed. In [26–28] the authors devise numerical schemes for finding approximate solutions of the Fokker-Planck Kolmogorov equation, thus allowing for the calculation of expected quantities, in particular the average harvested power. In [29–32] stochastic averaging of energy envelope methods are applied to find the system response and average output power. Alternatively, average quantities can be found by converting stochastic differential equations (SDEs) for the state variables into systems of ordinary differential equations (ODEs) for the expected quantities. For nonlinear systems, the ODE system is generally open, and *ad hoc* techniques must be applied to achieve closure [33,34].

In this work we investigate the role that nonlinearities and different types of white and colored stochastic sources, both additive and multiplicative, play in energy harvesting systems. One of the major differences with respect to the aforementioned works is that we study the effect of nonlinearities not only in the restoring elastic force, but also in the friction. The main finding is that for state dependent noise, nonlinear friction may significantly increase the harvester power, because it may induce bifurcations from low energy states (equilibrium points) to higher energy states (limit cycles). Another major contribution is the analysis technique, which is based on the transformation to energy-angle equations and the derivation of a reduced energy equation using projection operators. The method can be applied to both colored and white noise. We show that, in general, averaging the equations is not sufficient as memory effects must be taken into account. The method here presented allows for the derivation of a power balance equation (PBE), that can be used to calculate the energy probability density function and the average injected and extracted power, thus enabling a complete characterization of the harvester's performance. The PBE equation may also be exploited for design purposes to determine the harvester optimal working point.

2 System modeling

Irrespective of the details on the adopted power conversion mechanism, most energy harvesting systems rely upon oscillators to convert mechanical energy into electrical energy. As we consider a single DOF description, we describe a nonlinear oscillator for energy harvesting applications by means of the second order differential equation

$$\ddot{x} + V'(x) = f(x, \dot{x}, \xi(t)) \tag{1}$$

where x is the position (state) of the oscillator, dots denote derivative with respect to time, prime denotes derivative with respect to the argument and $\xi(t)$ represents the stochastic source. The second order differential equation (1) can be rewritten as a system of first order equations

$$\begin{cases} \dot{x} = y \\ \dot{y} = -V'(x) + f(x, y, \xi(t)) \end{cases} \tag{2}$$

Mechanical vibrations are usually limited in magnitude, thus it is legitimate to linearize (2) around the noiseless solution obtaining

$$\begin{cases} \dot{x} = y \\ \dot{y} = -V'(x) + f(x, y, 0) + \left.\dfrac{\partial f}{\partial \xi}\right|_{\xi=0} \xi(t) \end{cases} \quad (3)$$

In the absence of damping f and without noise, (3) describes a *Hamiltonian system*, i.e. a system with constant energy. Function $f(x, y, 0)$ collects the dissipation terms, such as internal friction, resistance in the circuitry, and the harvesting system that subtracts energy from the vibrating structure and converts it into usable power. Finally, $\partial f / \partial \xi$ is a modulating function since it is calculated for $\xi = 0$.

The energy of mechanical vibrations is spread over a wide range of frequencies, suggesting to model random vibrations as a white noise process. From the mathematical point of view, Gaussian white noise $\xi(t) = \dot{W}_t$ is characterized by zero expectation $\langle \dot{W}_t \rangle = 0$ and Dirac delta time correlation $\langle \dot{W}_t \dot{W}_s \rangle = \delta(t - s)$. White noise is a reasonable approximation in the case where the typical time scales of the underlying deterministic dynamics are much larger than the noise correlation time (quasi-white approximation).

When the quasi-white approximation does not apply, one must take into account the finite, non null noise correlation time, and that the power of random mechanical vibrations is concentrated at low frequency rather than being uniformly distributed on the whole frequency range. In this case a more appropriate model for the noise source is represented by an exponentially correlated process known as Ornstein-Uhlenbeck process (OUP). OUP $\xi(t) = \eta_t$ is the solution of the linear stochastic differential equation

$$\dot{\eta}_t = -k \, \eta_t + \overline{D} \, \dot{W}_t \quad (4)$$

where k is the drift coefficient, $\overline{D}$ is the diffusion constant and W_t is a Wiener process, i.e. the integral of a white noise. OUP with initial condition η_0 is characterized by the expectation value

$$\langle \eta_t \rangle = \langle \eta_0 \rangle e^{-kt} \quad (5)$$

and by the time correlation function

$$R(t, t + s) = \langle \eta_t \, \eta_{t+s} \rangle = \frac{\overline{D}}{k} e^{-k|s|} \quad (6)$$

The noise intensity for a process with non-negative time correlation function is defined by the time integral

$$N = \int_0^{+\infty} R(t, s) \, ds = \frac{\overline{D}^2}{k^2} \quad (7)$$

while the noise correlation time is

$$\tau = \int_0^{+\infty} \frac{R(t, s)}{R(t, 0)} \, ds = \frac{1}{k} \quad (8)$$

We begin considering the white noise source case, rewriting (3) as a set of stochastic differential equations (SDEs)

$$dx = y \, dt \quad (9a)$$

$$dy = [-V'(x) + \varepsilon_f f(x, y)] \, dt + \varepsilon_n \, D \, g(x, y) \, dW_t \quad (9b)$$

where we have introduced the parameters ε_f and ε_n (not necessarily small) to take into account friction and noise intensity, respectively. Because noise is modulated by function $g(x, y)$, the problem arises whether (9) should be interpreted as a Stratonovich or as an Itô SDE [35, 36]. For our purpose, it is convenient to interpret (9) as an Itô SDE.

Conversely, in the case noise is better approximated by a OUP, (3) becomes

$$dx = y \, dt \quad (10a)$$

$$dy = [-V'(x) + \varepsilon_f f(x, y) + \varepsilon_n \, g(x, y) \, \eta_t] \, dt \quad (10b)$$

$$d\eta_t = -\frac{\eta_t}{\tau} \, dt + \frac{D}{\tau} \, dW_t \quad (10c)$$

where we have rewritten (3) and (4) as SDEs and we have introduced the new parameter $D = \overline{D} \, \tau$.

It is worth noticing that in the (x, y, η_t) space, equation (10) describes a diffusion process with unmodulated white Gaussian noise, therefore its solution does not depend on the stochastic calculus interpretation being used. For analysis purposes, it is convenient to transform (10) into an equivalent system in a reduced space (x, y), subject to white Gaussian noise. By equivalent we mean that the transformed system retains the same statistical properties of the original system with colored noise. The advantage of this transformation is twofold: first it makes a direct comparison with system (9) immediate; second the same analysis technique can be used for both systems.

It can be shown (see [37,38]) that for short noise correlation time, the solution of the Itô SDE

$$dx = y \, dt \quad (11a)$$

$$dy = \left[-V'(x) + \varepsilon_f f(x, y) + \varepsilon_n^2 \frac{D^2}{2} g(x, y) \frac{\partial g(x, y)}{\partial y}\right] dt$$

$$+ \varepsilon_n D g(x, y) dW_t \quad (11b)$$

is also a weak solution of (10). That is, for a specific realization of the Wiener process W_t, the solutions of (10) and (11) differ in details but retain the same statistical

properties such as mean, variance and higher moments. This information is sufficient for most practical applications. Therefore we shall study the Itô SDE with a multiplicative noise source

$$\mathrm{d}x = y\,\mathrm{d}t \tag{12a}$$

$$\mathrm{d}y = \left[-V'(x) + \varepsilon_f f(x,y) + \varepsilon_n^2 h(x,y)\right]\mathrm{d}t$$
$$+ \varepsilon_n g(x,y)\mathrm{d}W_t \tag{12b}$$

where[1]

$$h(x,y) = \begin{cases} 0 & \text{for white noise} \\ \dfrac{1}{2}\,g(x,y)\dfrac{\partial g(x,y)}{\partial y} & \text{for colored noise} \end{cases} \tag{13}$$

3 Energy-angle representation

We are now going to rewrite the state equation (12) in terms of energy and angle variables. Stochastic differential equations for energy and angle can thus be derived, providing an ideal starting point for the analysis of the power injected into the system by noise and of the extracted power.

The total energy of the system is the sum of kinetic and potential energy components $E = y^2/2 + V(x)$. In the undamped and noiseless limit ($\varepsilon_f = \varepsilon_n = 0$), system (12) describe a Hamiltonian system that can be transformed into energy-angle coordinates so that the governing equations take the special form [39]

$$\dot{E} = 0 \tag{14a}$$

$$\dot{\theta} = \Omega(E) \tag{14b}$$

where θ is the angle function and $\Omega(E)$ is the angular frequency. Because the Jacobian of the coordinate transformation $(x,y) \rightarrow (E,\theta)$ is regular, by the implicit function theorem the coordinate transformation is invertible for small values of ε_f and ε_n, at least locally as in general a global change of coordinates is not guaranteed to exist.

In most practical problems, e.g. weakly nonlinear and/or anharmonic oscillators, the old coordinates can be expressed in terms of the new ones in the form $x = x(E,\theta)$, $y = y(E,\theta)$. Using Itô calculus and Itô lemma

[35,36] it is straightforward to derive a SDE for the energy

$$\mathrm{d}E = \left[\varepsilon_f a_E(E,\theta) + \varepsilon_n^2 b_E(E,\theta)\right]\mathrm{d}t$$
$$+ \varepsilon_n B_E(E,\theta)\mathrm{d}W_t \tag{15}$$

where (for the sake of simplicity, we use x, y to denote $x(E,\theta), y(E,\theta)$)

$$a_E(E,\theta) = y\,f(x,y) \tag{16a}$$

$$b_E(E,\theta) = \frac{1}{2}\,g^2(x,y) + y\,h(x,y) \tag{16b}$$

$$B_E(E,\theta) = y\,g(x,y) \tag{16c}$$

Derivation of the SDE for the angle variable is more involved. Two different situations can occur.

3.1 Angle equation given $\theta(x,y)$

The SDE for the angle is easily found if the expressions for $x(E,\theta)$ and $y(E,\theta)$ can be inverted to find an explicit formula for $\theta(x,y)$. Given the function $\theta(x,y)$, application of Itô formula and Itô lemma yields

$$\mathrm{d}\theta = \left[\Omega(E) + \varepsilon_f a_\theta(E,\theta) + \varepsilon_n^2 b_\theta(E,\theta)\right]\mathrm{d}t$$
$$+ \varepsilon_n B_\theta(E,\theta)\mathrm{d}W_t \tag{17}$$

where

$$\Omega(E) = \frac{\partial \theta}{\partial x}\,y - \frac{\partial \theta}{\partial y}V'(x) \tag{18a}$$

$$a_\theta(E,\theta) = \frac{\partial \theta}{\partial y}\,f(x,y) \tag{18b}$$

$$b_\theta(E,\theta) = \frac{1}{2}\,\frac{\partial^2 \theta}{\partial y^2}\,g^2(x,y) + \frac{\partial \theta}{\partial y}\,h(x,y) \tag{18c}$$

$$B_\theta(E,\theta) = \frac{\partial \theta}{\partial y}\,g(x,y) \tag{18d}$$

3.2 Angle equation given $x(E,\theta)$ and $y(E,\theta)$

Although theoretically feasible, in many practical problems inverting the expressions $x(E,\theta)$, and $y(E,\theta)$ to find an explicit relation for $\theta(x,y)$ may be difficult or at least unpractical, because $x(E,\theta)$ and $y(E,\theta)$ often involve special functions that are hard to handle.

If this is the case, one may proceed as follows. First we observe that for the undamped, noiseless system ($\varepsilon_f = \varepsilon_n = 0$), we have

$$\dot{x} = \frac{\partial x}{\partial E}\dot{E} + \frac{\partial x}{\partial \theta}\dot{\theta} \tag{19}$$

---

[1] Without loss of generality we shall assume $D = 1$. Different values of D can be taken into account by rescaling the noise intensity according to $\tilde{\varepsilon}_n = \varepsilon_n D = \varepsilon_n \overline{D}\tau$. Therefore, by varying the parameter ε_n we can investigate the influence of both the noise diffusion coefficient $\overline{D}$ and the noise correlation time τ.

that together with (14) yields

$$\dot{\theta} = \Omega(E) = \left(\frac{\partial x}{\partial \theta}\right)^{-1} y \tag{20}$$

In presence of dissipation and noise, from $x(E, \theta)$ and using Itô formula we obtain

$$dx = \frac{\partial x}{\partial E}dE + \frac{\partial x}{\partial \theta}d\theta + \frac{1}{2}\frac{\partial^2 x}{\partial E^2}(dE)^2 + \frac{1}{2}\frac{\partial^2 x}{\partial \theta^2}(d\theta)^2$$
$$+ \frac{\partial^2 x}{\partial E \partial \theta}dEd\theta \tag{21}$$

so that

$$d\theta = \left(\frac{\partial x}{\partial \theta}\right)^{-1}\left[dx - \frac{\partial x}{\partial E}dE - \frac{1}{2}\frac{\partial^2 x}{\partial E^2}(dE)^2\right.$$
$$\left. -\frac{1}{2}\frac{\partial^2 x}{\partial \theta^2}(d\theta)^2 - \frac{\partial^2 x}{\partial E \partial \theta}dEd\theta\right] \tag{22}$$

Equation (15), together with Itô lemma, implies

$$(dE)^2 = \varepsilon_n^2 B_E^2(E, \theta)dt \tag{23}$$

On the other hand, we expect also the angle to be an Itô process, so that

$$d\theta = \alpha(E, \theta)dt + \beta(E, \theta)dW_t \tag{24}$$

where $\alpha(E, \theta)$ and $\beta(E, \theta)$ are unknown functions to be determined. By Itô lemma

$$(d\theta)^2 = \beta^2(E, \theta)dt \tag{25}$$
$$dEd\theta = \varepsilon_n B_E(E, \theta)\beta(E, \theta)dt \tag{26}$$

Introducing (23)-(26) into (17) and equating the coefficients of dW_t we obtain

$$\beta(E, \theta) = -\varepsilon_n \left(\frac{\partial x}{\partial \theta}\right)^{-1}\frac{\partial x}{\partial E}B_E(E, \theta) \tag{27}$$

Finally, we can write the angle equation (17) where the coefficients are now given by

$$a_\theta(E, \theta) = -\left(\frac{\partial x}{\partial \theta}\right)^{-1}\frac{\partial x}{\partial E}a_E(E, \theta) \tag{28a}$$

$$b_\theta(E, \theta) = -\left(\frac{\partial x}{\partial \theta}\right)^{-1}\left[\frac{\partial x}{\partial E}b_E(E, \theta) + \frac{1}{2}\frac{\partial^2 x}{\partial E^2}B_E^2(E, \theta)\right.$$
$$\left. +\frac{1}{2}\frac{\partial^2 x}{\partial \theta^2}B_\theta^2(E, \theta) + \frac{\partial^2 x}{\partial E \partial \theta}B_E(E, \theta)B_\theta(E, \theta)\right] \tag{28b}$$

$$B_\theta(E, \theta) = -\left(\frac{\partial x}{\partial \theta}\right)^{-1}\frac{\partial x}{\partial E}B_E(E, \theta) \tag{28c}$$

4 Reduced energy equation

The SDEs for energy (15) and angle (17) are exact, as no approximation was introduced in their derivation, but in general they are not easier to solve than the original problem (12). Applying stochastic projection operator methods, in this section we derive a reduced SDE for the energy. Being single variable, the reduced equation can be analyzed to obtain the marginal probability density function for the energy.

The Fokker-Planck equation (FPE) associated to the energy-angle SDEs, whose unknown is the joint probability density function (PDF) $p(E, \theta, t)$ of the two variables, reads

$$\frac{\partial p(E, \theta, t)}{\partial t} = \left(\Lambda_0 + \varepsilon_f \Lambda_{\varepsilon_f} + \varepsilon_n^2 \Lambda_{\varepsilon_n}\right)p(E, \theta, t) \tag{29}$$

where we define $\Lambda = \Lambda_0 + \varepsilon_f \Lambda_{\varepsilon_f} + \varepsilon_n^2 \Lambda_{\varepsilon_n}$, and the three operators are

$$\Lambda_0 p = -\Omega(E)\frac{\partial p}{\partial \theta} \tag{30a}$$

$$\Lambda_{\varepsilon_f} p = -\frac{\partial}{\partial E}\left[a_E(E, \theta)p\right] - \frac{\partial}{\partial \theta}\left[a_\theta(E, \theta)p\right] \tag{30b}$$

$$\Lambda_{\varepsilon_n} p = -\frac{\partial}{\partial E}\left[b_E(E, \theta)p\right] - \frac{\partial}{\partial \theta}\left[b_\theta(E, \theta)p\right]$$
$$+ \frac{1}{2}\frac{\partial^2}{\partial E^2}\left[B_E^2 p\right] + \frac{1}{2}\frac{\partial^2}{\partial \theta^2}\left[B_\theta^2 p\right]$$
$$+ \frac{\partial^2}{\partial E \partial \theta}\left[B_E B_\theta p\right] \tag{30c}$$

The stationary distribution p_{st} for the zero-th order equation $\partial p/\partial t = \Lambda_0 p$ is independent on the angle, $p_{\text{st}} = p_{\text{st}}(E)$. Imposing the normalization condition

$$\int_0^{\Omega(E)T(E)} p_{\text{st}}(E)d\theta = 1 \tag{31}$$

we find

$$p_{\text{st}} = \frac{1}{\Omega(E)T(E)} \tag{32}$$

Here $\Omega(E)$ and $T(E)$ are the oscillator angular frequency and period, respectively. Thus $[0, \Omega(E)T(E)]$ is the angle range that, in the simplest case as, e.g., for linear oscillators, corresponds to $\Omega(E)T(E) = 2\pi$. However, for more complex nonlinear oscillators, different ranges may arise because of possible parametrizations of non circular oscillations (see later on in section 6).

The stationary distribution can be used to introduce a projection operator P, defined through its action over a generic function $F(E, \theta, t)$

$$PF(E, \theta, t) = p_{\text{st}}\int_0^{\Omega(E)T(E)} F(E, \theta, t)d\theta \tag{33}$$

The application of the projection operator to the PDF yields the marginal PDF for the energy $Pp(E,\theta,t) = \hat{p}(E,t)$. Together with P we define the complementary operator Q such that $P+Q=I$, where I is the identity operator.

Applying the two complementary projection operators to the FPE (29) we have

$$\frac{\partial}{\partial t}P\,p(E,\theta,t) = P\,\Lambda\,Pp(E,\theta,t) + P\,\Lambda\,Q\,p(E,\theta,t) \quad (34)$$

$$\frac{\partial}{\partial t}Q\,p(E,\theta,t) = Q\,\Lambda\,Pp(E,\theta,t) + Q\,\Lambda\,Q\,p(E,\theta,t) \quad (35)$$

At any time instant, the solution of (35) is in the null space of P. Because the equation is linear, a formal solution is

$$Q\,p(E,\theta,t) = e^{tQ\Lambda}Qp(E,\theta,0)$$
$$+ \int_0^t e^{(t-s)Q\Lambda}Q\Lambda Pp(E,\theta,s)\,\mathrm{d}s \quad (36)$$

Introducing (36) into (34) gives the Mori-Zwanzig equation

$$\frac{\partial Pp(E,\theta,0)}{\partial t} = P\Lambda Pp(E,\theta,t) + P\Lambda e^{tQ\Lambda}Q\,p(E,\theta,0)$$
$$+ P\Lambda \int_0^t e^{(t-s)Q\Lambda}Q\Lambda Pp(E,\theta,s)\,\mathrm{d}s \quad (37)$$

Without loss of generality, we can chose the initial distribution $p(E,\theta,0)$ in the null space of Q, thus making the second term on the right hand side of (37) null. The last term represents a memory effect, being the consequence of the attempt to follow the full dynamics looking only at a subset of variables [20]. The full system is Markovian, since the knowledge of the state at a given time permits to determine the state at any successive instant. However, if only a subset of variables is considered, the reduced system becomes non Markovian, and keeps track of the eliminated variables through the memory term. For the sake of simplicity, we shall assume that the memory effect becomes very quickly negligible, or, in other words, that the system has a very short time memory. Under this assumption the reduced FPE simplifies to

$$\frac{\partial Pp(E,\theta,0)}{\partial t} \approx P\left(\Lambda_0 + \varepsilon_f\Lambda_{\varepsilon_f} + \varepsilon_n^2\Lambda_{\varepsilon_n}\right)Pp(E,\theta,t) \quad (38)$$

Using (30) and (31), and imposing the periodic boundary conditions

$$p(E,0,t) = p(E,\Omega(E)T(E),t) \quad (39)$$

$$\frac{\partial p}{\partial \theta}(E,0,t) = \frac{\partial p}{\partial \theta}(E,\Omega(E)T(E),t) \quad (40)$$

a lengthy but straightforward calculation gives

$$P\Lambda_0 Pp(E,\theta,t) = 0 \quad (41a)$$

$$P\Lambda_{\varepsilon_f}Pp(E,\theta,t) = \frac{-1}{\Omega(E)T(E)}\frac{\partial}{\partial E}\left[\overline{a}_E(E)\hat{p}(E,t)\right] \quad (41b)$$

$$P\Lambda_{\varepsilon_n}Pp(E,\theta,t) = \frac{-1}{\Omega(E)T(E)}\frac{\partial}{\partial E}\left[\overline{b}_E(E)\hat{p}(E,t)\right]$$
$$+ \frac{1}{2\Omega(E)T(E)}\frac{\partial^2}{\partial E^2}\left[\overline{B}_E^2(E)\hat{p}(E,t)\right] \quad (41c)$$

where

$$\overline{a}_E(E) = \frac{1}{\Omega(E)T(E)}\int_0^{\Omega(E)T(E)} a_E(E,\theta)\,\mathrm{d}\theta \quad (42a)$$

$$\overline{b}_E(E) = \frac{1}{\Omega(E)T(E)}\int_0^{\Omega(E)T(E)} b_E(E,\theta)\,\mathrm{d}\theta \quad (42b)$$

$$\overline{B}_E(E) = \sqrt{\frac{1}{\Omega(E)T(E)}\int_0^{\Omega(E)T(E)} B_E^2(E,\theta)\,\mathrm{d}\theta} \quad (42c)$$

As a consequence the reduced FPE (38) for the marginal PDF $\hat{p}(E,t)$ is

$$\frac{\partial \hat{p}(E,t)}{\partial t} = -\frac{\partial}{\partial E}\left\{\left[\varepsilon_f\overline{a}_E(E) + \varepsilon_n^2\overline{b}_E(E)\right]\hat{p}(E,t)\right\}$$
$$+ \frac{\varepsilon_n^2}{2}\frac{\partial^2}{\partial E^2}\left[\overline{B}_E(E)\hat{p}(E,t)\right] \quad (43)$$

that corresponds to the reduced SDE for the energy

$$\mathrm{d}E = \left[\varepsilon_f\overline{a}_E(E) + \varepsilon_n^2\overline{b}_E(E)\right]\mathrm{d}t + \varepsilon_n\overline{B}_E(E)\mathrm{d}W_t \quad (44)$$

Notice that a reduced energy equation similar to (44) can be obtained by direct application of stochastic averaging to (15)–(17), under the hypothesis that a time scale separation exists between the fast (the angle) and the slow (the energy) variables [40,30,31,41,32]. This condition obviously is satisfied if $\varepsilon_n \ll \Omega(E)$ and $\varepsilon_f \ll \Omega(E)$. Contrary to stochastic averaging, where the time scale separation assumption is introduced since the very beginning, our derivation based on projection operators is exact (no approximations are made) up to the Mori-Zwanzig equation (37). This equation can thus be used as a starting point for further analysis, such as the investigation of memory terms effects on the dynamics, e.g. short memory (but not vanishing small) or long memory (t-model) [37].

5 Stationary marginal probability density function and power balance equation

The averaged FPE (43) is a single variable partial differential equation. The stationary solution $\hat{p}_{\mathrm{st}}(E)$ can

be easily found imposing $\partial \hat{p}/\partial t = 0$ together with null boundary conditions

$$\lim_{E \to +\infty} \hat{p}_{\text{st}}(E) = 0 \tag{45}$$

thereby obtaining

$$\hat{p}_{\text{st}}(E) = \frac{\mathcal{N}}{\overline{B}_E^2(E)} \exp\left(\frac{2}{\varepsilon_n^2} \int \frac{\varepsilon_f \overline{a}_E(E) + \varepsilon_n^2 \overline{b}_E(E)}{\overline{B}_E^2(E)} \, \mathrm{d}E\right) \tag{46}$$

where $\mathcal{N}$ is a constant that can be determined imposing the normalization condition $\int_0^{+\infty} \hat{p}_{\text{st}}(E) \, dE = 1$.

The most probable values of the energy (mode) correspond to the maxima of the stationary distribution, that is to the solution of the equation $\hat{p}'_{\text{st}}(E) = 0$. Taking the derivative of (46), the mode are among the solutions of the equation

$$\frac{2}{\varepsilon_n^2}\left[\varepsilon_f \overline{a}_E(E) + \varepsilon_n^2 \overline{b}_E(E)\right] - 2\overline{B}_E(E)\overline{B}'_E(E) = 0 \tag{47}$$

It is interesting to compare the mode with the equilibrium points of the damped, noiseless system, that are found solving

$$\overline{a}_E(E) = 0 \tag{48}$$

In general, the mode do not correspond to the equilibrium points. Therefore, noise influences the dynamics of the system in several ways. Not only it can shift the mode with respect to the equilibrium points, but it can also modify the stability of the solutions. For instance, under the influence of noise a system can begin to fluctuate around an unstable equilibrium point of the deterministic system, a phenomenon known as noise induced stability.

Another interesting phenomenon is a noise induced phase transition, i.e. noise may generate preferred points that do not have correspondence in the underlying deterministic system. These transitions correspond to a qualitative change of the probability distribution, that can for instance be modified from uni-modal to multi-modal as the noise intensity is varied.

Noise induced phenomena open interesting possibilities to the designer, who could in principle exploit noise induced transitions to design devices working at operating points not accessible to the deterministic systems. Another possibility would be to design systems that work at unstable equilibrium points. Here large deviations can be expected, as a result of the natural tendency of the system to escape from such unstable points, balanced by the noise that is continuously pushing the system towards the unstable equilibrium.

The power balance equation is obtained from (44) by taking the stochastic expectation on both sides and by using the zero expectation property of Itô stochastic integral

$$\left\langle \frac{dE}{dt} \right\rangle = \varepsilon_f \left\langle \overline{a}_E(E) \right\rangle + \varepsilon_n^2 \left\langle \overline{b}_E(E) \right\rangle \tag{49}$$

The left hand side of (49) represents the instantaneous expected power, while the expectations on the right hand side are the harvested and friction dissipated power, and the power injected into the system by noise, respectively. They are computed using the stationary PDF (46)

$$\left\langle \overline{a}_E(E) \right\rangle = \int_{-\infty}^{+\infty} \overline{a}_E(E)\, \hat{p}_{\text{st}}(E) \, \mathrm{d}E \tag{50}$$

$$\left\langle \overline{b}_E(E) \right\rangle = \int_{-\infty}^{+\infty} \overline{b}_E(E)\, \hat{p}_{\text{st}}(E) \, \mathrm{d}E \tag{51}$$

Asymptotically, the system reaches a steady state, i.e. an equilibrium point of the ODE (49). Such a state corresponds to the situation where the power injected by the noise into the system $P_{\text{in}} = \varepsilon_n^2 \langle \overline{b}_E(E) \rangle$ equals the power subtracted from the system by the harvesting mechanism and the internal friction $P_{\text{out}} = \varepsilon_f \langle \overline{a}_E(E) \rangle$. Since the injected and extracted powers depend on the energy level, it is in principle possible to maximize the harvested power by properly controlling the state of the system, thus making it possible to design a system with an optimized working point.

6 Influence of nonlinearity and correlation time

We shall now apply the theoretical tools developed in the previous sections to investigate the role of nonlinearities and noise correlation time on the power available in the harvesting system. We shall consider two types of nonlinear behavior: The first is a nonlinearity in the oscillator state equations as a consequence of the potential energy. Potential $V_1(x) = x^2/2$, and $V_2(x) = ax^2/2 + bx^4/4$ will be considered, describing a linear (LO) and a nonlinear oscillator (NLO), respectively.

Second, we shall consider both linear and nonlinear frictions, i.e. a simple linear friction (LF) term $f_a(x, y) = -y$, and a van der Pol-like nonlinear friction (NLF) $f_b(x, y) = (1 - x^2)y$.

Finally we shall assume that the noise modulation function is $g(x, y) = (1+y)$, implying that noise is both additive and multiplicative. As a consequence, the additional drift term (13) is $h_\alpha(x, y) = 0$ for white noise (WDR), and $h_\beta(x, y) = (1 + y)/2$ for colored noise (CDR). The coefficients for the complete energy SDE (15), including the diffusion noise term, as given by (16), are summarized in Table 1.

Table 1 Coefficients for the full energy SDE (10). Cases of the LF/NLF LO/NLO oscillators, WDR/CDR noise, diffusion noise

LF	$a_E^{(a)}(x,y) = -y^2$
NLF	$a_E^{(b)}(x,y) = (1-x^2)y^2$
WDR	$b_E^{(\alpha)}(x,y) = (1+y)^2/2$
CDR	$b_E^{(\beta)}(x,y) = (1+3y+2y^2)/2$
Diffusion	$B_E(x,y) = (1+y)y$

Table 2 Coefficients for the reduced energy SDE (44) for the LO. Cases of LF/NLF, WDR/CDR noise, diffusion noise

LF	$\overline{a}_E^{(a)}(E) = -E$
NLF	$\overline{a}_E^{(b)}(E) = E - E^2/2$
WDR	$\overline{b}_E^{(\alpha)}(E) = (1+E)/2$
CDR	$\overline{b}_E^{(\beta)}(E) = (1+2E)/2$
Diffusion	$\overline{B}_E(E) = \sqrt{3E^2/2 + E}$

6.1 Linear oscillator (LO)

First we consider an energy harvester based on a linear oscillator. The potential energy in this case is simply $V_1(x) = x^2/2$. Position and velocity coordinates can be written as functions of energy and angle in the form

$$x = \sqrt{2E}\sin\theta, \quad y = \sqrt{2E}\cos\theta \tag{52}$$

where $\theta \in (0, 2\pi)$. Using (20) we have the angular frequency $\Omega(E) = 1$ and period $T(E) = 2\pi$ for all initial conditions[2]. The coefficients of the reduced SDE for the energy (44) are easily computed through (42) and are summarized in Table 2.

It is worth noticing that taking the stochastic expectation for $\overline{b}_E(E)$ in Table 2, we find that the noise injected power is proportional to the expected energy: $P_{\text{in}} \propto \varepsilon_n^2 \langle E \rangle$. This result is what suggested to use a van der Pol-like friction (NLF), as the latter may give advantages with respect to the LF case.

In presence of linear dissipation, the oscillator exhibits noise induced random fluctuations around a stable equilibrium point (the origin). By converse, the NLF LO oscillator fluctuates around a stable limit cycle. Since the latter corresponds to a higher energy level than the former, the noise injected power will be increased.

The stationary PDFs are found from (46): The results are summarized in Table 3.

---

[2] The corresponding phase portrait is known as *isochronous center*

Table 3 Stationary reduced energy PDF for the LO. Cases of LF/NLF, WDR/CDR noise

LF, WDR	$p_{\text{st}} = N(3E+2)^{-\frac{4\varepsilon_f + 4\varepsilon_n^2}{3\varepsilon_n^2}}$
NLF, WDR	$p_{\text{st}} = N(3E+2)^{\frac{16\varepsilon_f - 12\varepsilon_n^2}{9\varepsilon_n^2}} e^{-\frac{2\varepsilon_f}{3\varepsilon_n^2}(3E+2)}$
LF, CDR	$p_{\text{st}} = N(3E+2)^{-\frac{4\varepsilon_f + 2\varepsilon_n^2}{3\varepsilon_n^2}}$
NLF, CDR	$p_{\text{st}} = N(3E+2)^{\frac{16\varepsilon_f - 6\varepsilon_n^2}{9\varepsilon_n^2}} e^{-\frac{2\varepsilon_f}{9\varepsilon_n^2}(3E+2)}$

Figure 1 shows the stationary PDF $p_{\text{st}}(x,y)$ for the linear oscillator with white and colored noise, obtained through numerical integration of (9) and (10). The Euler-Maruyama numerical integration scheme was used, with time integration step $\Delta t = 20 \times 10^{-6}$, and simulation length $\Delta T = 10^5$. The probability to find the system in the state $x+dx, y+dy$ has been computed as the number of samples in such an interval, normalized to the total sample number. For comparison, an approximation for $p_{\text{st}}(x,y)$ can be found under the hypothesis that, because of the time scale separation, angle and energy become independent variables. Thus it is legitimate to assume $p_{\text{st}}(x,y) = p_{\text{st}}(\theta)\hat{p}_{\text{st}}(E)$. Using (32) and remembering that $E = y^2/2 + V(x)$ we have

$$p_{\text{st}}(x,y) = \frac{1}{\Omega(E)T(E)}\hat{p}_{\text{st}}(E) \tag{53}$$

Theoretical predictions given by (53) are shown in figure 2.

Figure 3 shows the marginal PDF for the energy of a linear oscillator with white and colored noise. Stationary PDFs obtained from numerical integration of (9) and (10) are compared with the theoretical PDFs shown in Table 3.

6.2 Nonlinear oscillator

We choose a nonlinear oscillator characterized by the potential energy $V_2(x) = ax^2/2 + bx^4/4$ where a and b are real, positive parameters. Position and velocity coordinates can be written as functions of energy and angle in the form

$$x = \left(\frac{4E^2}{a^2 + 4bE}\right)^{1/4} \text{sd}(\theta, k) \tag{54a}$$

$$y = \sqrt{2E}\, \text{cd}(\theta, k)\, \text{nd}(\theta, k) \tag{54b}$$

where $\text{sd}(\theta,k)$, $\text{cd}(\theta,k)$ and $\text{nd}(\theta,k)$ are Jacobi elliptic functions and

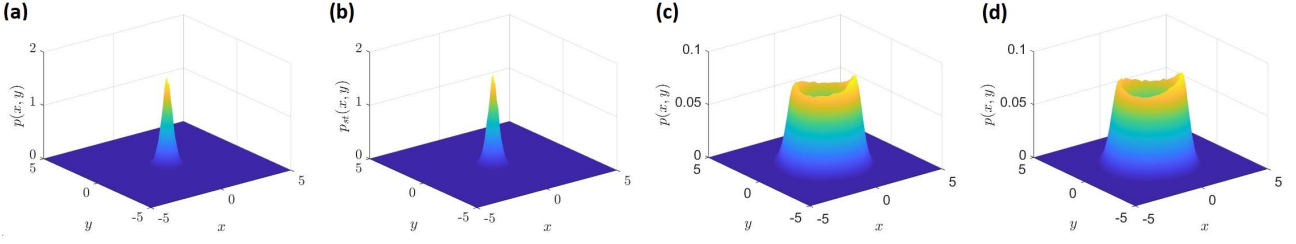$$k^2 = \frac{1}{2}\left(1 - \frac{a}{\sqrt{a^2 + 4bE}}\right) \tag{55}$$

Fig. 1 PDF for a linear oscillator subject to white and colored noise. Parameters are $\varepsilon_f = 0.05$ and $\varepsilon_n = 0.10$. Correlation time for the Ornstein-Uhlenbeck process is $\tau = 0.25$. **(a)** Linear friction, white noise. **(b)** Linear friction, colored noise. **(c)** Nonlinear friction, white noise. **(d)** Nonlinear friction, colored noise.
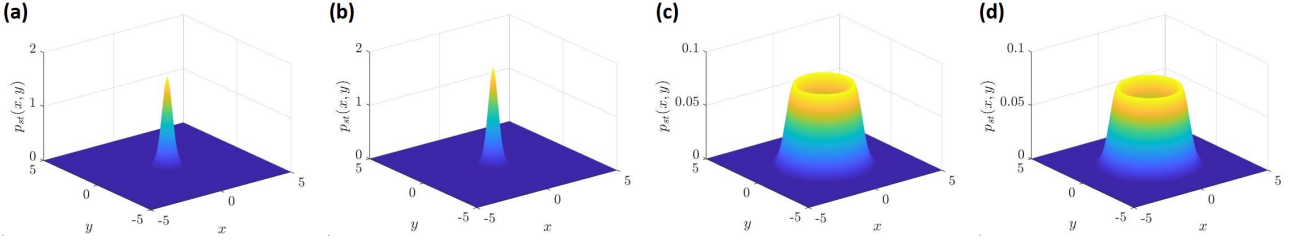

Fig. 2 Theoretical prediction for the PDF of a linear oscillator subject to white and colored noise. Parameters are $\varepsilon_f = 0.05$ and $\varepsilon_n = 0.10$. Correlation time for the Ornstein-Uhlenbeck process is $\tau = 0.25$. **(a)** Linear friction, white noise. **(b)** Linear friction, colored noise. **(c)** Nonlinear friction, white noise. **(d)** Nonlinear friction, colored noise.
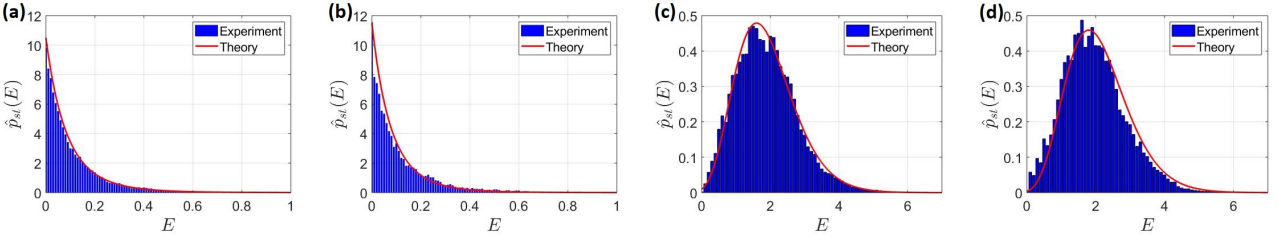

Fig. 3 Theoretical prediction for the marginal PDF for the energy of a linear oscillator subject to white and colored noise. Parameters are $\varepsilon_f = 0.05$ and $\varepsilon_n = 0.10$. Correlation time for the Ornstein-Uhlenbeck process is $\tau = 0.25$. Blue vertical bars are results of numerical experiments. Solid red line is the theoretical prediction. **(a)** Linear friction, white noise. **(b)** Linear friction, colored noise. **(c)** Nonlinear friction, white noise. **(d)** Nonlinear friction, colored noise.

is the elliptic modulus [42]. Here $\theta \in (0, 4\mathcal{K}(E))$, where $\mathcal{K}(E)$ denotes the complete elliptic integral of the first kind [42]. Using (20) we find the angular frequency $\Omega(E) = (a^2 + 4bE)^{1/4}$.

The coefficients of the reduced energy SDE (44) are shown in Table 4, where $k'^2 = 1 - k^2$ is the complementary modulus [42], and $I_n(E)$ denote the integral function[3]

$$I_n = \int \mathrm{nd}^n u \, \mathrm{d}u \qquad (56)$$

Figure 4 shows the stationary PDFs for the nonlinear oscillator subject to white and colored noise, computed through numerical integration of (9) and (10), respectively. The marginal energy stationary PDFs are shown in Figure 5, where they are compared against

---

[3] Analytical formulas in terms of complete elliptic integrals and elliptic modulus for these integral functions are given in the appendix.

Table 4 Coefficients for the reduced energy SDE (44) for the NLO. Cases of LF/NLF, WDR/CDR noise, diffusion noise

LF	$\overline{a}_E^{(a)}(E) = -\dfrac{E}{2\mathcal{K}} \left(\dfrac{1}{k^2} I_2 - \dfrac{k'^2}{k^2} I_4 \right)$
NLF	$\overline{a}_E^{(b)}(E) = \dfrac{E}{2\mathcal{K}} \left(\dfrac{1}{k^2} I_2 - \dfrac{k'^2}{k^2} I_4 \right)$
	$\quad + \dfrac{E^2}{\mathcal{K}\sqrt{a^2 + 4bE^2}} \left(\dfrac{k'^2}{k^2} I_6 - \dfrac{k'^2 + 1}{k^4} I_4 \right.$
	$\quad \left. + \dfrac{1}{k^4} I_2 \right)$
WDR	$\overline{b}_E^{(\alpha)}(E) = \dfrac{1}{2} + \dfrac{E}{4\mathcal{K}} \left(\dfrac{1}{k^2} I_2 - \dfrac{k'^2}{k^2} I_4 \right)$
CDR	$\overline{b}_E^{(\beta)}(E) = \dfrac{1}{2} + \dfrac{E}{2\mathcal{K}} \left(\dfrac{1}{k^2} I_2 - \dfrac{k'^2}{k^2} I_4 \right)$
Diffusion	$\overline{B}_E(E) = \left[\dfrac{E}{2\mathcal{K}} \left(\dfrac{1}{k^2} I_2 - \dfrac{k'^2}{k^2} I_4 \right) \right.$
	$\quad \left. + \dfrac{E^2}{\mathcal{K}} \left(\dfrac{k'^4}{k^4} I_8 - \dfrac{2k'^2}{k^4} I_6 + \dfrac{1}{k^4} I_4 \right) \right]^{1/2}$

the theoretical prediction (46). For the nonlinear case, we are not able to give analytical expressions for $\hat{p}_{st}(E)$, however we did integrate numerically (46) using the coefficients in Table 4.

We can now investigate the role of nonlinearity on the injected and extracted power. Figure 6 shows a comparison between the stationary PDFs for the LO and NLO based energy harvesting system. The upper graph shows that in the case of linear friction, as far as the stationary PDF is concerned there are no significant differences between linear and nonlinear oscillators. Noise correlation time also does not seem to play a significant role, because the difference between the PDFs for white and colored noise is minimal. The situation is very different in the case of nonlinear friction (shown below). In the NLF case, the stationary marginal PDF for the energy of LO is very different from that of NLO. Also, noise correlation plays a significant role, as the PDF for colored noise is rather different from that of white noise of the same intensity.

Finally, figure 7 shows the power injected by noise (both white and colored) into a linear and a nonlinear oscillator-based energy harvesting system. The injected power has been evaluated implementing (51) exploiting the $\bar{b}_E$ reported in Table 2 and the stationary PDF in Table 3 (solid lines). The theoretical results are validated against the numerically computed injected power evaluated from (9) and (11). Above we show the power injected in the case of linear friction. For both white and colored noise there is no advantage in using a nonlinear oscillator rather than a linear one (blue/red and black/green lines are superimposed). This result can be explained as follows: weak noise induces fluctuations around the origin, the unique, asymptotically stable equilibrium point, that are too small to initiate significant nonlinear effects. In the case of linear friction, colored noise sources provide slightly more power than WDR sources of the same intensity.

The situation is very much different for the case of nonlinear friction (lower figure part). Here nonlinear oscillators outperform linear ones for both white and colored noise sources. Furthermore, energy harvesting systems with nonlinear friction perform significantly better, by almost an order of magnitude, than those based on linear friction.

As mentioned above, for this specific example the better harvesting performance of the nonlinear friction device are due to the modulated noise component. In fact, since the power injected by noise is proportional to the energy level, the working point fluctuating around a limit cycle outperforms a device operated around the origin as the former corresponds to a larger energy.

7 Conclusions

We have presented a novel procedure for reducing the stochastic equations describing the dynamics of a single DOF stochastic energy harvesting system subject to white and time-correlated noise sources. After transforming the state variable description into energy angle-variables, through stochastic projection and averaging we have obtained a power balance equation that puts in evidence the importance of nonlinear elements and noise correlation time on the energy harvesting performance.

Exploiting the PBE, we have shown that nonlinear energy harvesters subject to modulated (multiplicative) stochastic sources can outperform their linear counterparts, thus opening the way to exploiting nonlinear dynamic analysis techniques for the possible improvement of energy harvesting systems.

A Solution of the nonlinear oscillator

In absence of noise and for the potential $V(x) = ax^2/2 + bx^4/4$ equation (2) becomes

$$\dot{x} = y$$
$$\dot{y} = -ax - bx^3$$

Dividing one equation by the other, separating variables and integrating one finds

$$\frac{y^2}{2} + a\frac{x^2}{2} + b\frac{x^4}{4} = H_0$$

where H_0 is a constant representing the energy. Solving with respect to y and considering only the positive determination yields

$$y = \sqrt{4H_0 - 2ax^2 - bx^4}$$

Substituting in $\dot{x} = y$ and separating variables gives the first order differential equation

$$\frac{\mathrm{d}x}{\sqrt{4H_0 - 2ax^2 - bx^4}} = \mathrm{d}t$$

Integrating both sides it turns out that $x(t)$ is in fact given by [43]

$$x(t) = \left(\frac{4E^2}{a^2 + 4bE}\right)^{1/4} \mathrm{sd}[(a^2 + 4bE)^{1/4}t, k]$$

where $E = 4H_0$ represents the energy level. Differentiating with respect to time

$$y(t) = \sqrt{2E}\,\mathrm{cd}[(a^2 + 4bE)^{1/4}t, k]\,\mathrm{nd}[(a^2 + 4bE)^{1/4}t, k]$$
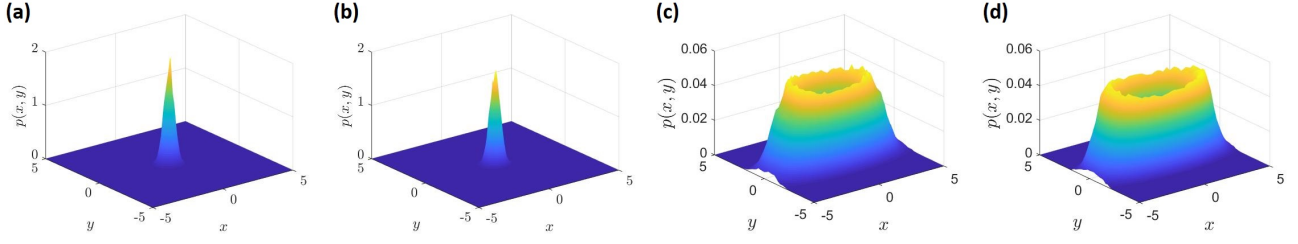
Fig. 4 Probability density function for a nonlinear oscillator with nonlinear potential $V(x) = x^2/2 + x^4/4$. Parameters are $\varepsilon_f = 0.05$ and $\varepsilon_n = 0.10$. Correlation time for the Ornstein-Uhlenbeck process is $\tau = 0.25$. **(a)** Linear friction, white noise. **(b)** Linear friction, colored noise. **(c)** Nonlinear friction, white noise. **(d)** Nonlinear friction, colored noise.
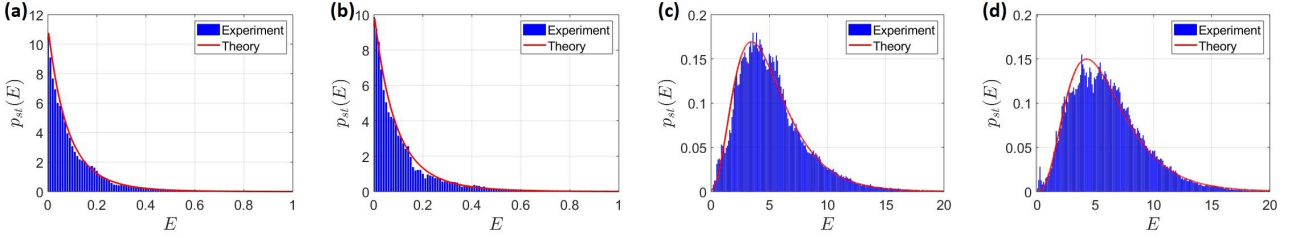

Fig. 5 Theoretical prediction for the marginal PDF for the energy of a nonlinear oscillator with nonlinear potential $V(x) = x^2/2 + x^4/4$. Parameters are $\varepsilon_f = 0.05$ and $\varepsilon_n = 0.10$. Correlation time for the Ornstein-Uhlenbeck process is $\tau = 0.25$. Blue vertical bars are results of numerical experiments. Solid red line is the theoretical prediction. **(a)** Linear friction, white noise. **(b)** Linear friction, colored noise. **(c)** Nonlinear friction, white noise. **(d)** Nonlinear friction, colored noise.
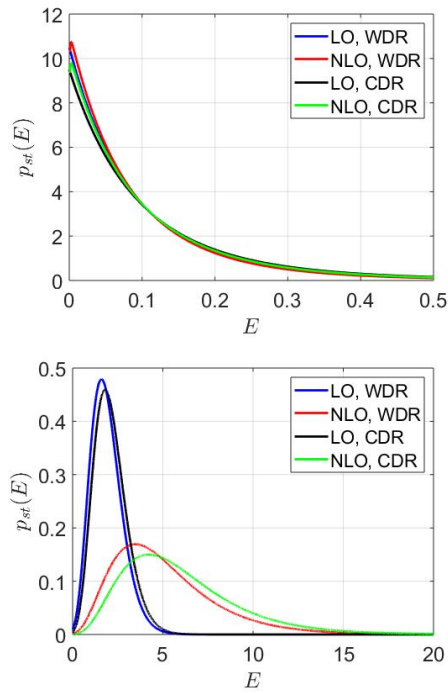

Fig. 6 Comparison between stationary marginal PDFs of a linear and a nonlinear oscillator subject to white and colored noise. Parameters are $\varepsilon_f = 0.05$ and $\varepsilon_n = 0.10$. Correlation time for the Ornstein-Uhlenbeck process is $\tau = 0.25$. Above: PDFs for a linear oscillator (LO) and a nonlinear oscillator (NLO) subject to both white (WDR) and colored (CDR) noise, in the case of linear friction. Below: same as above but for nonlinear friction.
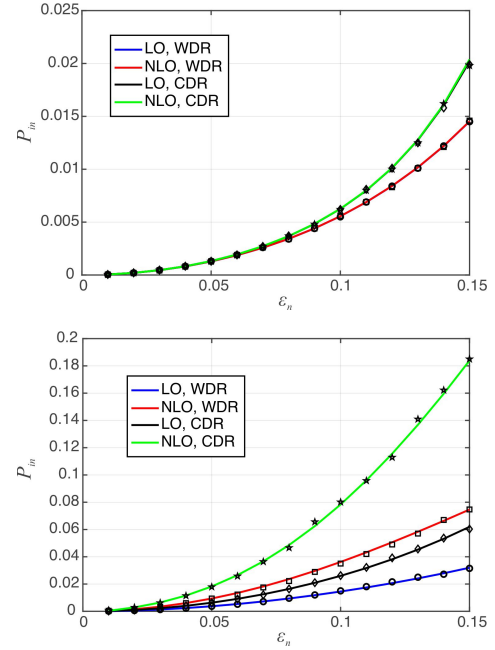

Fig. 7 Comparison between the power injected by noise for both linear (LO) and nonlinear (NLO) oscillator based harvesting system, as a function of the noise intensity. Both white (WDR) and colored noise (CDR) are considered. Parameters are $\varepsilon_f = 0.05$, noise correlation time for the Ornstein-Uhlenbeck process is $\tau = 0.25$. Above: Linear friction (LF). Below: Nonlinear friction (NLF). Solid line: Theoretical results. Symbols: numerical solution of the stochastic systems.

B Integral functions I_n

The well known relationships between the squares of Jacobi elliptic functions

$$k^2 \operatorname{sd}^2 u = \operatorname{nd}^2 u - 1$$

$$k^2 \operatorname{cd}^2 u = 1 - k'^2 \operatorname{nd}^2 u$$

imply that (42) can be reduced to the solution of the integrals

$$I_n = \int_0^{4\mathcal{K}(E)} \operatorname{nd}^n u \, \mathrm{d}u$$

For $n = 2, 4$ the integrals are easily computed with the help of the Fourier series for $\operatorname{nd}^2 u$ and $\operatorname{nd}^4 u$ [44], obtaining

$$I_2 = \int_0^{4\mathcal{K}(E)} \operatorname{nd}^2 u \, \mathrm{d}u = \frac{4\mathcal{E}(k)}{k'^2}$$

$$I_4 = \int_0^{4\mathcal{K}(E)} \operatorname{nd}^4 u \, \mathrm{d}u = \frac{8(2 - k^2)\mathcal{E} - 4(1 - k^2)\mathcal{K}}{3k'^4}$$

where $\mathcal{E}(k)$ is the complete elliptic integral of the second kind.

For larger values of n, integrals I_n can be computed using a recursive relation. Following the procedure described in [45] we find

$$\frac{\mathrm{d}}{\mathrm{d}u} \left(\operatorname{nd}^l u \operatorname{sd} u \operatorname{cd} u \right) = -(l + 2) \frac{k'^2}{k^2} \operatorname{nd}^{l+3} u$$

$$+ (l + 1) \frac{k'^2 + 1}{k^2} \operatorname{nd}^{l+1} u - l \frac{1}{k^2} \operatorname{nd}^{l-1} u$$

For $l = n - 3$

$$\frac{\mathrm{d}}{\mathrm{d}u} \left(\operatorname{nd}^{n-3} u \operatorname{sd} u \operatorname{cd} u \right) = (1 - n) \frac{k'^2}{k^2} \operatorname{nd}^n u$$

$$+ (n - 2) \frac{k'^2 + 1}{k^2} \operatorname{nd}^{n-2} u - (3 - n) \frac{1}{k^2} \operatorname{nd}^{n-4} u$$

Integrating and rearranging terms

$$I_n = \frac{1}{(1 - n)k'^2} \left[(2 - n)(k'^2 + 1)I_{n-2} + (n - 3)I_{n-4} \right]$$

Conflict of Interest

The authors declare that they have no conflict of interest.

References

1. Kurs, A., Karalis, A., Moffatt, R., Joannopoulos, J.D., Fisher, P., Soljačić, M.: Wireless power transfer via strongly coupled magnetic resonances. Science **317**(5834), 83–86 (2007). DOI 10.1126/science.1143254
2. Cannon, B.L., Hoburg, J.F., Stancil, D.D., Goldstein, S.C.: Magnetic resonant coupling as a potential means for wireless power transfer to multiple small receivers. IEEE Transactions on Power Electronics **24**(7), 1819–1825 (2009). DOI 10.1109/tpel.2009.2017195
3. Sample, A.P., Meyer, D.A., Smith, J.R.: Analysis, experimental results, and range adaptation of magnetically coupled resonators for wireless power transfer. IEEE Transactions on Industrial Electronics **58**(2), 544–554 (2011). DOI 10.1109/tie.2010.2046002
4. Beeby, S.P., Tudor, M.J., White, N.M.: Energy harvesting vibration sources for microsystems applications. Measurement Science and Technology **17**(12), R175–R195 (2006). DOI 10.1088/0957-0233/17/12/r01
5. Mitcheson, P., Yeatman, E., Rao, G., Holmes, A., Green, T.: Energy harvesting from human and machine motion for wireless electronic devices. Proceedings of the IEEE **96**(9), 1457–1486 (2008). DOI 10.1109/jproc.2008.927494
6. Lu, X., Wang, P., Niyato, D., Kim, D.I., Han, Z.: Wireless networks with RF energy harvesting: A contemporary survey. IEEE Communications Surveys & Tutorials **17**(2), 757–789 (2015). DOI 10.1109/comst.2014.2368999
7. Roundy, S., Wright, P.K., Rabaey, J.M.: Energy Scavenging for Wireless Sensor Networks. Springer US (2004). DOI 10.1007/978-1-4615-0485-6
8. Paradiso, J., Starner, T.: Energy scavenging for mobile and wireless electronics. IEEE Pervasive Computing **4**(1), 18–27 (2005). DOI 10.1109/mprv.2005.9
9. Meninger, S., Mur-Miranda, J., Amirtharajah, R., Chandrakasan, A., Lang, J.: Vibration-to-electric energy conversion. IEEE Transactions on Very Large Scale Integration (VLSI) Systems **9**(1), 64–76 (2001). DOI 10.1109/92.920820
10. Mitcheson, P., Green, T., Yeatman, E., Holmes, A.: Architectures for vibration-driven micropower generators. Journal of Microelectromechanical Systems **13**(3), 429–440 (2004). DOI 10.1109/jmems.2004.830151
11. Anton, S.R., Sodano, H.A.: A review of power harvesting using piezoelectric materials (2003–2006). Smart Materials and Structures **16**(3), R1–R21 (2007). DOI 10.1088/0964-1726/16/3/r01
12. Cottone, F., Vocca, H., Gammaitoni, L.: Nonlinear energy harvesting. Physical Review Letters **102**(8) (2009). DOI 10.1103/physrevlett.102.080601
13. Gammaitoni, L., Neri, I., Vocca, H.: Nonlinear oscillators for vibration energy harvesting. Applied Physics Letters **94**(16), 164102 (2009). DOI 10.1063/1.3120279
14. Mann, B., Sims, N.: Energy harvesting from the nonlinear oscillations of magnetic levitation. Journal of Sound and Vibration **319**(1-2), 515–530 (2009). DOI 10.1016/j.jsv.2008.06.011
15. Gammaitoni, L., Neri, I., Vocca, H.: The benefits of noise and nonlinearity: Extracting energy from random vibrations. Chemical Physics **375**(2), 435–438 (2010). DOI 10.1016/j.chemphys.2010.08.012
16. Daqaq, M.F.: Response of uni-modal Duffing-type harvesters to random forced excitations. Journal of sound and Vibration **329**(18), 3621–3631 (2010). DOI 10.1016/j.jsv.2010.04.002
17. Neri, I., Travasso, F., Vocca, H., Gammaitoni, L.: Nonlinear noise harvesters for nanosensors. Nano Communication Networks **2**(4), 230–234 (2011). DOI 10.1016/j.nancom.2011.09.001
18. Masana, R., Daqaq, M.F.: Relative performance of a vibratory energy harvester in mono-and bi-stable potentials. Journal of Sound and Vibration **330**(24), 6036–6052 (2011). DOI 10.1016/j.jsv.2011.07.031
19. Gammaitoni, L.: There's plenty of energy at the bottom (micro and nano scale nonlinear noise harvesting). Contemporary Physics **53**(2), 119–135 (2012). DOI 10.1080/00107514.2011.647793
20. Bonnin, M., Corinto, F.: Phase noise and noise induced frequency shift in stochastic nonlinear oscillators. IEEE Transactions on Circuits and Systems I: Regular Papers **60**(8), 2104–2115 (August 2013). DOI 10.1109/TCSI.2013.2239131

21. Bonnin, M.: Amplitude and phase dynamics of noisy oscillators. International Journal of Circuit Theory and Applications **45**(5), 636–659 (2016). DOI 10.1002/cta.2246
22. Bonnin, M., Traversa, F.L., Bonani, F.: Influence of amplitude fluctuations on the noise-induced frequency shift of noisy oscillators. IEEE Transactions on Circuits and Systems II: Express Briefs **63**(7), 698–702 (2016). DOI 10.1109/tcsii.2016.2532098
23. Antoniadis, I., Venetsanos, D., Papaspyridis, F.: Dynamic non-linear energy absorbers based on properly stretched in-plane elastomer structures. Nonlinear Dynamics **75**(1-2), 367–386 (2014). DOI 10.1007/s11071-013-1072-8
24. Zhou, S., Cao, J., Lin, J.: Theoretical analysis and experimental verification for improving energy harvesting performance of nonlinear monostable energy harvesters. Nonlinear Dynamics **86**(3), 1599–1611 (2016). DOI 10.1007/s11071-016-2979-7
25. Serdukova, L., Kuske, R., Yurchenko, D.: Stability and bifurcation analysis of the period-T motion of a vibroimpact energy harvester. Nonlinear Dynamics pp. 1–13 (2019). DOI 10.1007/s11071-019-05289-8
26. Baratta, A., Zuccaro, G.: Analysis of nonlinear oscillators under stochastic excitation by the Fokker-Planck-Kolmogorov equation. Nonlinear Dynamics **5**(3), 255–271 (1994). DOI 10.1007/BF00045336
27. Guo, S.S.: Nonstationary solutions of nonlinear dynamical systems excited by Gaussian white noise. Nonlinear Dynamics **92**(2), 613–626 (2018). DOI 10.1007/s11071-018-4078-4
28. Meimaris, A.T., Kougioumtzoglou, I.A., Pantelous, A.A., Pirrotta, A.: An approximate technique for determining in closed form the response transition probability density function of diverse nonlinear/hysteretic oscillators. Nonlinear Dynamics **97**(4), 2627–2641 (2019). DOI 10.1007/s11071-019-05152-w
29. Zhu, W., Huang, Z., Suzuki, Y.: Response and stability of strongly non-linear oscillators under wide-band random excitation. International Journal of Non-Linear Mechanics **36**(8), 1235–1250 (2001). DOI 10.1016/S0020-7462(00)00093-7
30. Xu, M., Jin, X., Wang, Y., Huang, Z.: Stochastic averaging for nonlinear vibration energy harvesting system. Nonlinear Dynamics **78**(2), 1451–1459 (2014). DOI 10.1007/s11071-014-1527-6
31. Xiao, S., Jin, Y.: Response analysis of the piezoelectric energy harvester under correlated white noise. Nonlinear Dynamics **90**(3), 2069–2082 (2017). DOI 10.1007/s11071-017-3784-7
32. Zhang, Y., Jin, Y.: Stochastic dynamics of a piezoelectric energy harvester with correlated colored noises from rotational environment. Nonlinear Dynamics **98**(1), 501–515 (2019). DOI 10.1007/s11071-019-05208-x
33. Makarem, H., Pishkenari, H.N., Vossoughi, G.: A modified Gaussian moment closure method for nonlinear stochastic differential equations. Nonlinear Dynamics **89**(4), 2609–2620 (2017). DOI 10.1007/s11071-017-3608-9
34. Makarem, H., Pishkenari, H., Vossoughi, G.: A quasi-Gaussian approximation method for the Duffing oscillator with colored additive random excitation. Nonlinear Dynamics **96**(2), 825–835 (2019). DOI 10.1007/s11071-019-04824-x
35. Gardiner, C.W., et al.: Handbook of stochastic methods, vol. 3. Springer Berlin (1985)
36. Øksendal, B.: Stochastic Differential Equations, 6th edn. Springer–Verlag, Berlin (2003)
37. Givon, D., Kupferman, R., Stuart, A.: Extracting macroscopic dynamics: model problems and algorithms. Nonlinearity **17**(6), R55 (2004). DOI 10.1088/0951-7715/17/6/R01
38. Pavliotis, G., Stuart, A.: Multiscale methods: averaging and homogenization. Springer Science & Business Media (2008)
39. Goldstein, H., Poole, C., Safko, J.: Classical mechanics. AAPT (2002)
40. Khasminskij, R.: On the principle of averaging the Ito's stochastic differential equations. Kybernetika **4**(3), 260–279 (1968)
41. Zhang, Y., Jin, Y., Xu, P., Xiao, S.: Stochastic bifurcations in a nonlinear tristable energy harvester under colored noise. Nonlinear Dynamics pp. 1–19 (2018). DOI 10.1007/s11071-018-4702-3
42. Abramowitz, M., Stegun, I.A.: Handbook of mathematical functions: with formulas, graphs, and mathematical tables, vol. 55. Courier Corporation (1965)
43. Byrd, P.F., Friedman, M.D.: Handbook of elliptic integrals for engineers and physicists, vol. 67. Springer (2013)
44. Shi-Dong, W., Ji-Bin, L.: Fourier series of rational fractions of Jacobian elliptic functions. Applied Mathematics and Mechanics **9**(6), 541–556 (1988). DOI 10.1007/BF02465410
45. Savov, V., Georgiev, Z.D., Todorov, T.: Analysis and synthesis of perturbed Duffing oscillators. International journal of circuit theory and applications **34**(3), 281–306 (2006). DOI 10.1002/cta.351